Supplemental Document

Optics Letters

One-step formation of a plasmonic grating with an ultranarrow resonance linewidth for sensing: supplement

ZHIGANG HE, GUOGUO KANG,* JUNYI WANG, NING DING, AND YUWEI CHAI

School of Optoelectronics, Beijing Institute of Technology, Beijing 100081, China
Corresponding author: kgg@bit.edu.cn

Supplement DOI: https://doi.org/10.6084/m9.figshare.20032694

Parent Article DOI: https://doi.org/10.1364/OL.463866

One-step formation of plasmonic grating with ultranarrow resonance linewidth for sensing

ZHIGANG HE, GUOGUO KANG *, JUNYI WANG, NING DING, AND YUWEI CHAI

[1] *School of optics & electronics, Beijing Institute of Technology, Beijing 100081, China*
**Corresponding author: kgg@bit.edu.cn*

Received XX Month XXXX; revised XX Month, XXXX; accepted XX Month XXXX; posted XX Month XXXX (Doc. ID XXXXX); published XX Month XXXX

This document provides supplementary information to "One-step formation of plasmonic grating with ultranarrow resonance linewidth for sensing".

1. The dispersion properties of the materials of grating

We use an ellipsometer (VASE, J. A. Woollam) to measure the actual refractive index of Cu, photoresist and Au which are used in this paper. We will describe how to use this machine in section 6. The specific data of the refractive index are shown in Fig.S1.

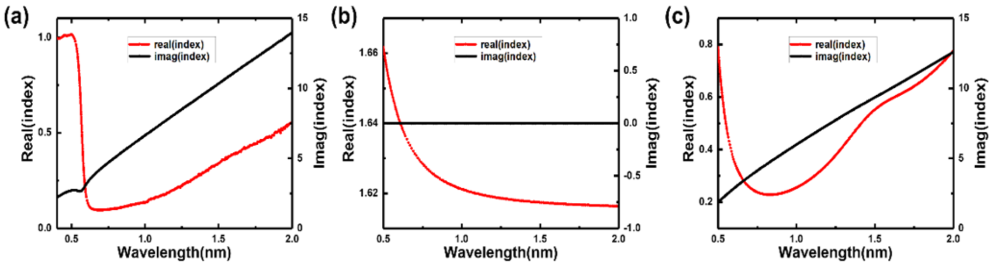

Fig. S1. The real and imaginary parts of the refractive index of (a) Cu and (b) the AZ5214E photoresist and (c) Au

2. The analysis of grating height and duty cycle

Here, we explain why we set the duty cycle F = 0.5 and grating height h = 100 nm. We fix the P as 600 nm and the incident angle θ as 15°. When the LIL exposure system is set up, the change of duty cycle will seriously affect the steepness of the grating. So, we set the F = 0.5, which is best for our existing exposure system. We scan h from 80 nm to 120 nm with a step of 10 nm, as is shown in fig. S2. With increasing height, the left dip is suppressed and the right dip becomes sharper. When the h reaches up to more than 100 nm, the change of the right dip becomes slow. We want both dips to have good performance, so we set F = 0.5 and h = 100 nm, which we think are most suitable for our design.

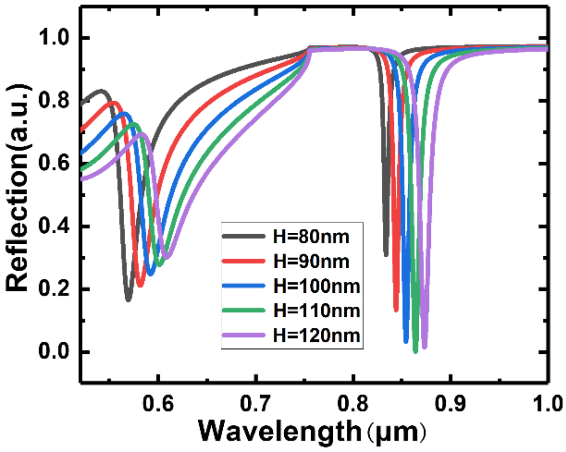

Fig. S2. The simulated reflective spectra of DGC-SPR sensor with various grating heights.

3. The choice of the materials of the metal substrate

In general, commonly used metals in plasmonic sensors are gold, silver, copper and aluminum. It is obvious that aluminum is highly oxidizing and silver plasmonic sensors work mostly not in visible or near-infrared bands. Considering all aspects, gold and copper are ideal composing materials for the metal substrate. We compared the performance of our DGC-SPR sensor with gold and copper substrate.

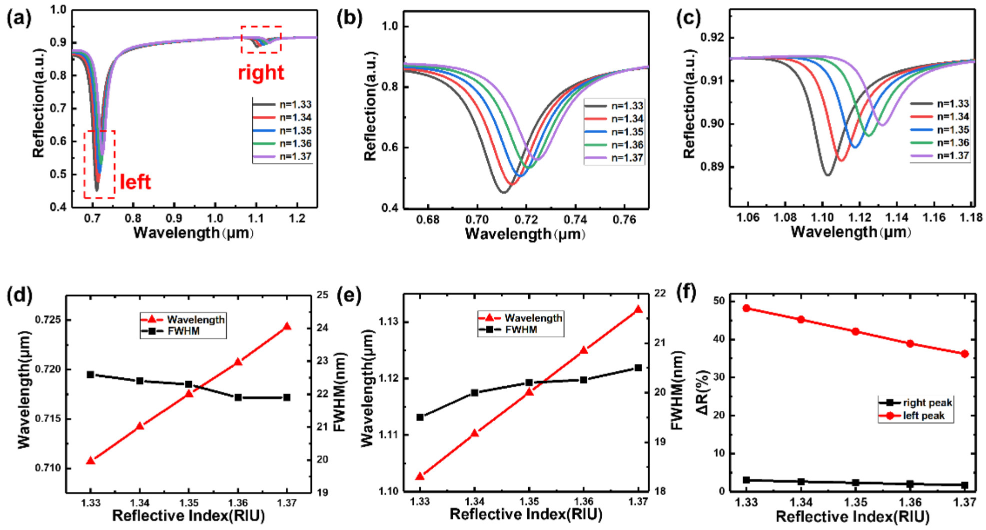

Fig. S3. (a) The simulated reflective spectra of DGC-SPR sensor (Au) with various ambient RIs. The partial enlarged drawing of (b) the left dip group (Au) and (c) the right dip group (Au). The resonance wavelength and FWHM of (d) the left dip group (Au) and (e) the right dip group (Au). (d) The ΔR of the two dip groups (Au).

As is shown in fig. S3, we simulated the sensing performance of the sensor with the gold substrate under the same grating and incidence light parameters. From fig. S3(b-c) and fig. S3(d-e), we can get the S of the left dip group (Au) being 340 nm/RIU and the right group (Au) 738 nm/RIU. Furthermore, the average FWHM of the left group (Au) is 22.2 nm and the right dip group (Au) is 20.1 nm. According to the definition of the FoM, the FoM of the two groups are 15.3 and 36.7, respectively. As shown in fig. S3(f), the left dip group has a significant advantage in the ΔR of which are ~20 times greater than the right. The trend of simulation data is similar, when Au and Cu are used as substrates respectively. For better illustration, we compare the simulation results of two cases in Table S1. The wavelength sensitivity (S) of gold is close to that of copper. However, the FWHM of the copper structure has been greatly optimized, which is almost half of the gold structure. In conclusion, considering the performance comparison between the sensors with gold and copper substrate and the cost, we chose Cu as the composing material of the metal substrate.

Table S1. The Performance of Cu Compared with Au

	left dip (Au)	left dip (Cu)	right dip (Au)	right dip (Cu)
S (nm/RIU)	340	**327**	738	**715**
FWHM (nm)	22.2	**7.8**	20.1	**5.5**
FoM (RIU^{-1})	15.3	**41.8**	36.7	**140.7**

4. The experimental system of exposure

The schematic diagram of the optical setup is shown in fig. S4. Firstly, a semiconductor laser (BCL-050-405-S, CrystaLaser, λ = 405 nm) is used as the light source[1]. The long propagation distance before the reflection mirror guarantees an acceptable beam profile considering the non-ideal performance of the semiconductor laser. The light passing through the hole is equivalent to a classical point light source. After the propagation distance of 1.5 m, the spot will spread far enough to cover the exposure area.

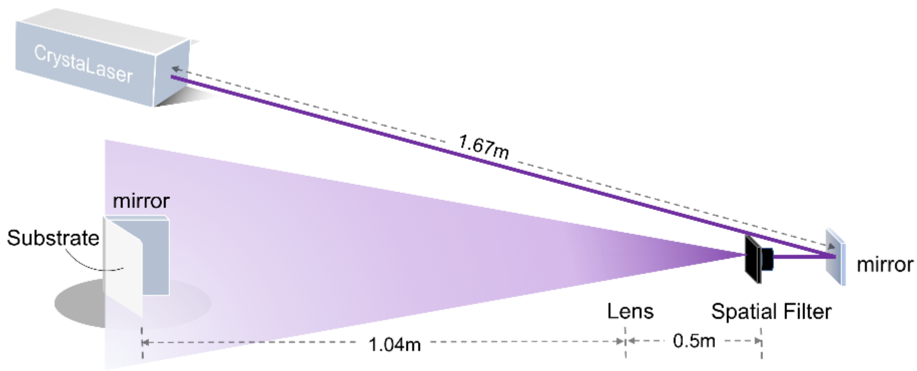

Fig. S4. Optical path schematic diagram.

5. The stability of DGC-SPR sensor

In order to investigate the stability of our sensor against analyte environment, we carried out experiments in which the sensor was fully immersed in glucose analyte with dose of 0.9g/20ml for 48 hours. Every 12 hours, we measured the reflection spectrum of our sensor with an incident angle of 15°. As is shown in fig. S5, the dips of the four measurements are basically the same, and the resonance band and FWHM are very stable. This shows that the sensor has good stability and is possible of being developed into a replaceable disposable consumable, considering its low cost and recycling capability.

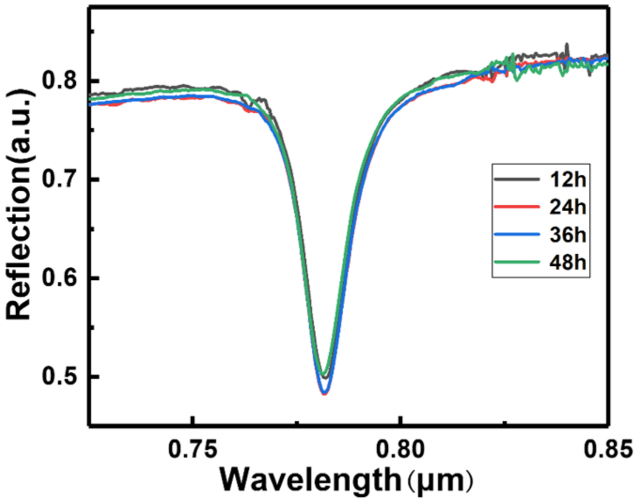

Fig. S5. The experimental reflective spectra of the sample in 48 hours.

6. The measurement equipment for the glucose RI and the performance of DGC-SPR sensor

In the manuscript, our sensing performance has been tested using a glucose solution as analyte. We used an Abbemat 450 refractometer from Anton Paar to measure the RI of the glucose solution. We simply drop the solvent into the test port, as is shown in fig. S6(a). The refractive index results will be displayed on the screen in fig. S6(b). The instrument is capable of measuring refractive index ranging from 1.26 to 1.72.

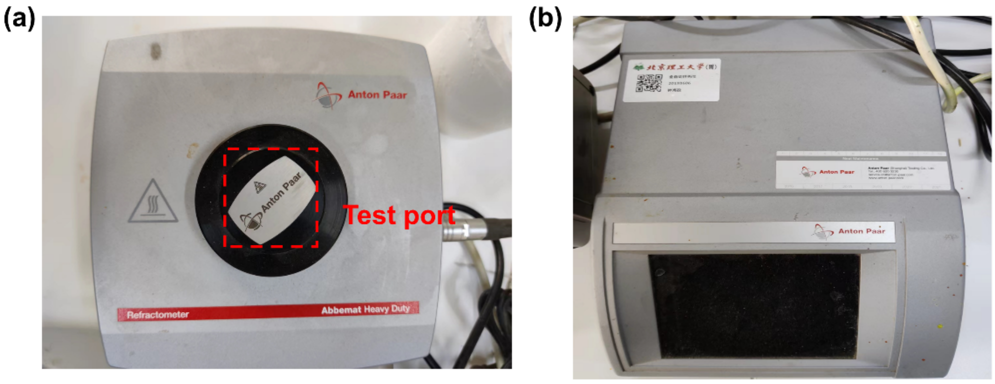

Fig. S6. (a) The test port of the Abbemat 450 (b) The display screen of Abbemat 450

The refractive sensing performance of DGC-SPR sensor is done by measuring the varied reflection spectra of the sensor when immersed in glucose solution with different doses. The relation of glucose solution doses with their RIs can be given by using the Abbemat 450 refractometer mentioned above. The reflection spectra of each solution are measured with an ellipsometer (VASE, J. A. Woollam), as is shown in fig. S7(a). The spectral range of light source can be set as 180-3300 nm, with minimum interval as 0.1 nm. The incident angle can be varied from 15° to 90° and the detector can capture the zero-order diffraction spectra. Then, the fabricated grating is placed in a homemade plastic tank and attached to the sample stage of the ellipsometer. The plastic tank is composed of a glass slide and a cover glass with interval of 1.3 mm in Fig. S7(b). The solution can be easily exchanged by firstly flushing out the current solution with deionized water and then adding new solutions into the cell. The ellipsometry data can also be used to calculate the refractive index of the measured material. The metal and photoresist samples can be attached to the sample stage of the ellipsometer. We also use the ellipsometer to measure the actual refractive index of the materials of grating in section 1.

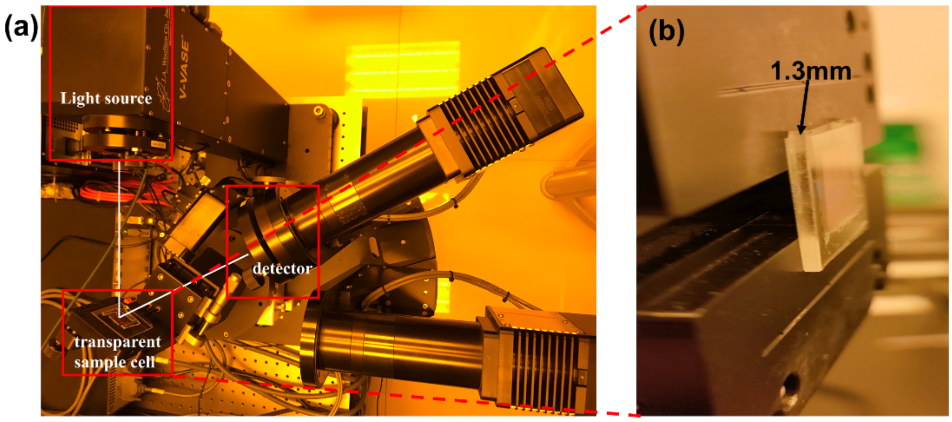

Fig. S7. (a) The ellipsometer (b) the homemade plastic tank.

References

1. I. Byun, and J. Kim, Journal of Micromechanics and Microengineering **20**, 055024 (2010).